Design of a Shack Hartmann Sensor, Vrns 2

Tilt Measurements

April 3, 2018

Introduction:

In Astronomy Notebook Section XVIII, pg 191, dated January 17, 2014 with conclusion on pg 217 we found surprisingly that the usual centroid or C-tilt was the least effective of several algorithms for reducing tip/tilt jitter, with peak detection being the best. Then we designed a Shack Hartman sensor, build a Reconstruction matrix, took videos of the Hartmann spots from which wavefront OPD was reconstructed. Then in Astronomy Notebook Section VII, pg 93, dated March 23, 2015 with conclusion on pg 115 we simulated the tip/tilt servo using the reconstructed wavefront from the movies and found that servoing off of Z-tilt gave the best jitter mitigating result.Z

Relevant Literature

Relevant to this study is the dissertation by John Paul Siegenthaler, GUIDELINES FOR ADAPTIVE-OPTIC CORRECTION BASED ON APERTURE FILTRATION , December 2008. It is worth noting his discussion in Chapter 3, page 49 regarding tilt. He writes,

3.2.1. Definitions of Tilt

As noted, the purpose of tilt correction is to remove net tilt from a wavefront and center the far-field pattern. However, "tilt" and "center" are not as clearly defined as one might think. Huygens' Principle defines tilt and a vector of propagation locally at each point in a wavefront. For tilt of a wavefront as a whole, there are two prevalent definitions.

Gradient-tilt, or G-tilt, is an average of all the local gradients on a wavefront, based on the assumption that an average of all the local propagation vectors on a wavefront should yield an average vector of propagation for the entire wavefront.[2] Zernike-tilt, or Z-tilt, comes from the set of Zernike polynomials that are often used to construct approximations of wavefronts and other surfaces. The Z_1^1 and Z_1^{-1} Zernike polynomials are of the form $z = r\cos(\theta)$ and $z = r\sin(\theta)$ respectively, or $z = x$ and $z = y$ in Cartesian coordinates. The polynomial Z_0 is of the form $z = 1$. Therefore, using the first three Zernike polynomials to approximate a wavefront takes the form of a least squares fit to a flat line $(A + Bx)$ in two-dimensional constructions or a plane $(A + Bx + Cy)$ in three-dimensional approximations.[3] As the desired end result of AO correction is a flat line or planar surface that is perpendicular to the desired vector of propagation, one

might expect that applying correction to remove the slope of this approximation to be an effective first step in achieving this.

However, as can be seen in Fig. 3.2, these two forms of tilt do not necessarily agree. Using a full cycle of a sine wave as a simulated wavefront, the average of the local propagation vectors is a vector perpendicular to the x-axis, which indicates no net angle of deflection and no net tilt. On the other hand, a least-squares fit with a function of the form y = A + B·x shows a significant slope across the extent of this wavefront, indicating tilt.

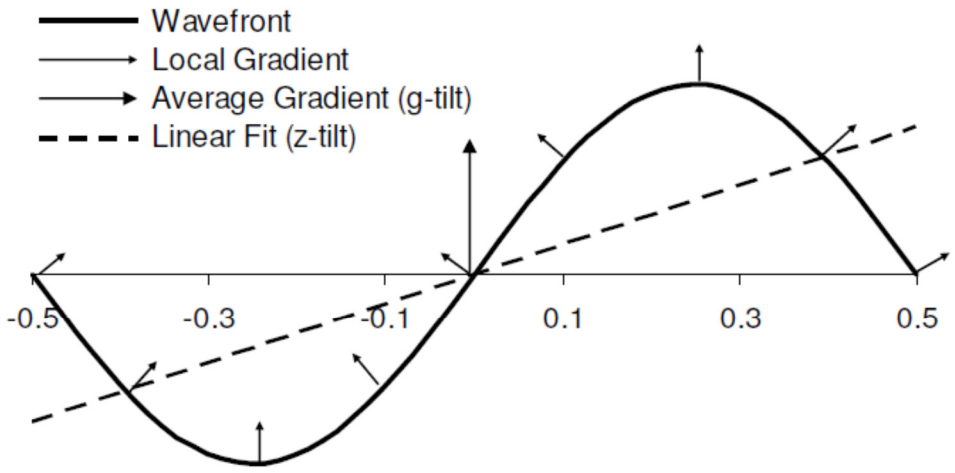

Figure 3.2: G-tilt defined by averaging local tilt, Vs Z-tilt defined by a linear fit.

Either definition of tilt may be considered to be correct, depending on the intended application.

G-tilt is the average of the deflection angles or slopes across a wavefront. If the wavefront is of uniform irradiance and is defined by a surface z(x) across a finite aperture extending from x_1 to x_2, then the x-component of G-tilt is defined by

$$G-Tilt_x = \int_{x_1}^{x_2} \frac{dz}{dx}\,dx \Big/ \int_{x_1}^{x_2} dx = \frac{z(x_2)-z(x_1)}{x_2-x_1}. \qquad (3.1)$$

Thus, for a wavefront of uniform irradiance over a one-dimensional aperture, G-tilt can be found by drawing a line between the endpoints of the wavefront at the edges of an aperture. In the example of Fig. 3.2, these endpoints are on a sine wave, separated by one full cycle, so $z(x_2) = z(x_1)$ and the G-tilt = 0. This property could be used as a means of detecting tilt across an aperture by measuring phase or OPD around the edges of an aperture.

Z-tilt is found by selecting constants A and B to minimize the expression

$$\int_{x_1}^{x_2} (z(x) - A - B \cdot x)^2 dx \,. \tag{3.2}$$

The value of B then corresponds to the overall tilt of the wavefront by this definition. If the point of reference is shifted so that the aperture of width d is centered around x = 0,

$$A = \frac{\int_{-d/2}^{d/2} z(x)dx}{d} \tag{3.3}$$

and

$$B = \frac{12 \int_{-d/2}^{d/2} x \cdot z(x)dx}{d^3} \,. \tag{3.4}$$

In the example of Fig. 3.2, if the sine wave used to represent a wavefront has an amplitude of a and a period of Λ, then

$$B = \frac{12 \int_{-d/2}^{d/2} x \cdot a \sin(2\pi/\Lambda\, x)dx}{d^3} = \frac{6a\left(2 \sin d\pi/\Lambda - d \cos d\pi/\Lambda\right)}{d^3 \pi} \,. \tag{3.5}$$

These expressions ignore variations in y, or cases in which irradiance is not constant in the near field. In cases with varying irradiance, such as that in a Gaussian beam, the wavefront displacement, z(x), must be weighted by the irradiance in the wavefront at that point. [4]

3.2.2. Measuring Tilt

While tilt can be inferred from the near-field wavefront as indicated in the preceding paragraphs, the most common means of measuring tilt is to find the center of the irradiance pattern in the far field. The point of T/T correction is to align the beam onto a target, thus the angle between the intended axis of propagation and the vector pointing to the center of the far-field pattern is a very practical definition of tilt.

This angle is most often found with some form of position sensing device, which receives an optical intensity pattern, and returns a value based on the position of the center of this pattern. If the irradiance pattern of a beam is found to be centered at (x_c, y_c) *while the desired*

on-axis location would be (0, 0), and it is known that the deflection occurred at some distance L from the sensor, then the angle of deflection (x) can be found to be

$$\theta_x = \arctan\left(x_c/L\right) \cong x_c/L \,, \theta_y = \arctan\left(y_c/L\right) \cong y_c/L \,. \tag{3.6}$$

The approximations $\theta_x \cong x_c/L$ *and* $\theta_y \cong y_c/L$ *hold if* x_c *and* $y_c \ll L$.

However, just as there is more than one definition of tilt for a wavefront, there is more than one way of defining the center of an irradiance pattern. This is illustrated by the two most common types of position sensors, quad cells and centroiding devices.

The four-element quadrant detector, or quad cell, is a set of four irradiance sensors, often some form of photodiode.[1] Arranged into a four-quadrant pattern, each cell produces a signal proportional to the total energy flux due to light falling on that cell. A representation of this arrangement is shown in Fig. 3.3. If we let A, B, C, and D represent the signals from these cells, then for small variations in from a centered position, the x-position of the irradiance pattern will be proportional to the quantity((A + B)− (C + D)) (A + B + C + D) . That is, the pattern is held to be centered at x = 0 when the total energy falling on the left half of the quad cell equals the total energy falling on the right half. Scaling the difference in energy falling on the two halves by the total energy falling on the entire sensor produces a result that will be proportional to the lateral shift in the pattern, with a constant of proportionality that will remain roughly the same even if there are changes in the pattern or overall irradiance. A similar relation holds for the y-position.

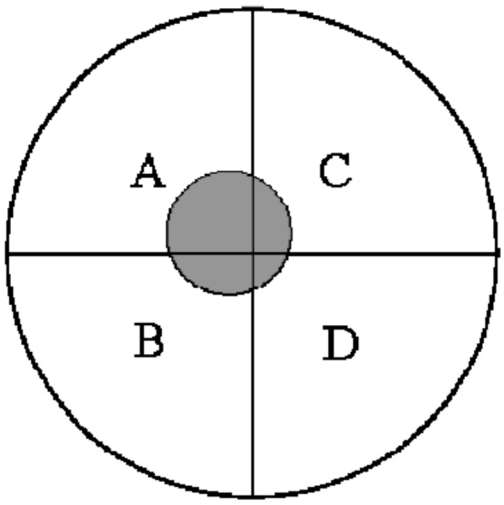

Figure 3.3: Sensor regions of a quad cell.

As noted, the proportionality for shifts in the location of the irradiance pattern only applies if that location is near to the center of the sensor, compared to the size of the pattern or the size of the central spot of the pattern if it has one. If a significant majority of the light falling on the sensor falls into one cell, the sensor has no way of telling where in the cell this concentration of incoming energy may be. A quad cell works best when the size of the sensor is only slightly larger than the size of the pattern for which a location is to be found. If the pattern is larger than the sensor, then significant portions of the light in the pattern may miss the sensor and will not be accounted for. If the pattern is small enough to fit into one cell, then the dynamic range of the sensor will be limited. Despite these limitations, quad cells are commonly used because their relative simplicity lends itself to implementations that are reliable and durable when used in the field.

Another type of position sensor is the lateral effect detector, which is also known as a position sensing device. This sensor consists of a sheet of photoelectric material with electrodes along the four sides of the sheet,[5] as shown in Fig. 3.4. When photons strike the photoelectric material, free electrons are produced that flow into the electrodes. The number of electrons produced at a point on the sensor is determined by the energy flux density of the light falling on that point. Some of the electrons produced then become current flowing into the four electrodes. These free electrons are more likely to flow into the electrode closest to their point of generation. If the light were focused to an infinitesimal spot, then the position of that spot between electrodes A and B in Fig. 3.4 would be proportional to the difference in the current flowing into A and the current flowing into B, divided by the sum of the two currents. That is, $x \propto {(A-B)}/{(A+B)}$ *where A and B are the currents flowing into the respective electrodes. A similar relation holds for the vertical position between electrodes C and D.*

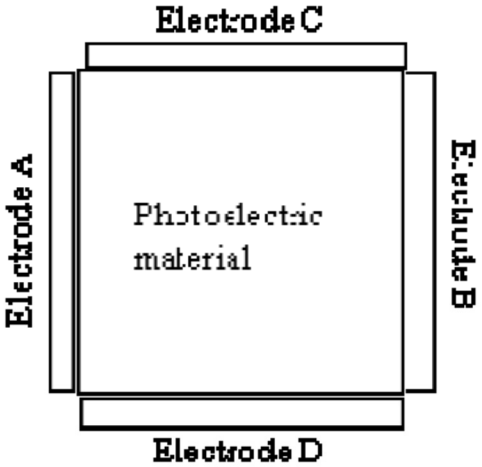

Figure 3.4: Components and arrangement of a Lateral Effect Detector sensor.

At first glance, this appears to be equivalent to the operation of the quad cell. However, when the energy within the intensity pattern is not concentrated on a single point, then a sensor of this sort will produce a result based on a weighted-average centroid of the form,

$$x_c = \frac{\iint x \cdot I(x, y)\, dx\, dy}{\iint I(x, y)\, dx\, dy}. \tag{3.7}$$

with a similar relationship for position in y. Since each point on the sensing area of the detector effectively acts as a separate sensor, this type of sensor is not as susceptible to considerations of pattern size or larger pattern shifts as the quad cell.

These different definitions of the center of an irradiance pattern are all quite valid, just as the different definitions of tilt in section 3.2.1 are valid. However, they are different, and if one does not keep those differences in mind, then that can lead to problems in trying to deal with tilt.

As tilt is primarily of interest in aligning the far-field intensity pattern on a target, a look at the far-field pattern is instructive. Figure 3.5 shows far-field intensity patterns for the sinusoidal wavefront in Fig. 3.2, with a peak-to-valley phase variance of 0.8 radians. The solid vertical line in Fig. 3.5 (a) indicates the location of the far-field intensity pattern's centroid, as found with a weighted average of the form in Eq. 3.7. The dashed vertical line in Fig. 3.5 (a) indicates the point corresponding to a quad cell definition of center, at which the total intensity to the left of that point $\sum I_x -$ equals the total intensity to the right of that point $\sum I_x +$.

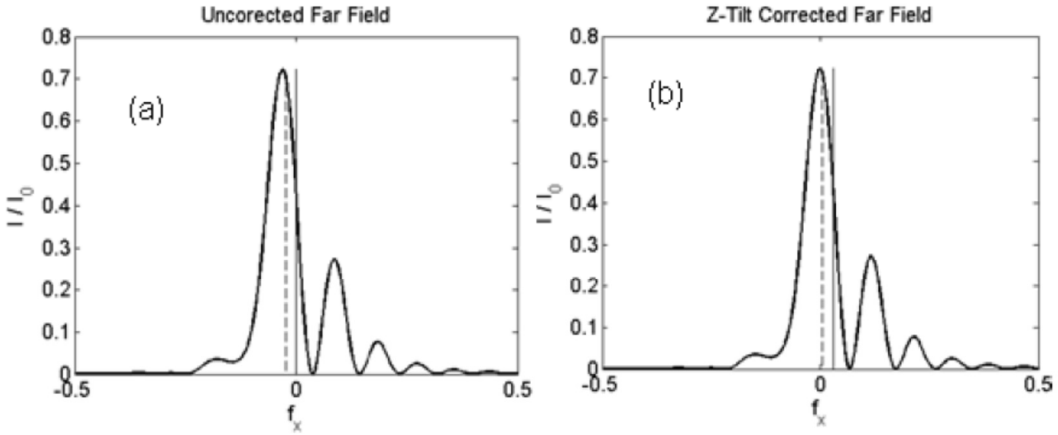

Figure 3.5: A far-field irradiance pattern based on a sinusoidal wavefront (a) and this pattern if the wavefront is corrected according to Z-tilt.

As can be seen in Fig. 3.5, the locations of these two definitions of the center are not equivalent. The centroid definition of centering the pattern is at x = 0, which indicates there was

no tilt in the original wavefront and agrees with earlier evaluation of G-tilt for the wavefront in Fig. 3.2. On the other hand, Fig. 3.5 (b) shows the far field for a wavefront with tilt calculated according to the Z-tilt definition and removed. Performing T/T correction based on this definition of tilt shifts the far-field pattern so that the center point according to the quad cell definition of center is placed near x = 0. Interestingly, this also places the point of highest intensity in the far field closer to x = 0.

Increasingly, arrays of charge-coupled device (CCD) photosensors, of the sort that serve as the basis for most digital cameras, have been used as position sensors.1 Each pixel in the array produces a signal or digital value proportional to the irradiance falling on that sensor. If a far-field pattern falls across several pixels of the array, then a weighted average centroid can be found through numerical integration approximating Eq.3.7. If the size of the pattern is on the order of one or two cells across, then a set of four pixels in a square pattern can be used as a quad cell. Larger blocks of pixels can be used as the equivalent of larger quad cells, but it is rare to do so if enough pixels are involved to make centroiding a viable option.

A limitation of CCD array centroiding is that spatial and temporal resolutions become factors in this form of sensor. Properly approximating Eq. 3.7 requires pixels small enough to resolve relevant features in the far-field pattern and enough pixels to encompass the pattern, including spreading and wandering of the pattern due to aberrations. As noted, four pixels that are larger than or on the order of the pattern size can be used in the manner of a quad-cell, but as it has also been noted, quad-cells and centroiding sensors have different definitions of tilt. The use of pixels of intermediate size will produce measured values of tilt that do not properly correspond to either Z-tilt or G-tilt, but are likely to lie somewhere between the two.

Quad cells and lateral effect detectors output only four signals. Those four signals are reduced to two values for tilt in x and y through operations of addition, subtraction, and division that are simple enough to be carried out by analog circuitry. Each pixel in a CCD outputs a separate signal that must be read and recorded in order to perform the calculations. The computation to convert these values into T/T is also more involved than that for quad cells and lateral effect detectors. The time required to read in all values and perform the computation can limit the sampling rate for a CCD-based sensor.

Before leaving this discussion, it should be noted that recognition of the difference in G and Z-tilt and their ramifications to tilt correction were derived independently during work that will be described in chapter 8. As presented here, the implications of tilt measurement and correction at first glance appear as only subtleties, but in practice they have very real unintended consequences. Through further study, it became apparent that G and Z-tilt are well-established phenomena and, in that sense, this discovery amounted to rediscovering the wheel.

References

[1] Tyson, R.K., *Principles of Adaptive Optics*, Academic Press, San Diego, 1991
[2] Tyson, R.K. (editor), *Adaptive Optics Engineering Handbook*, Ch. 3, R.J. Sasiela and J.D. Shelton, *Guide Star System Considerations*, Marcel Dekker, New York, 2000.

[3] Sasiela, R.J, *Electromagnetic Wave Propagation in Turbulence: Evaluation and Application of Mellin Transforms*, SPIE Press, 2007.
[4] Barchers, J.D., Fried, D.L., Link, D.J., Evaluation of the performance of Hartmann sensors in strong scintillation, *Applied Optics*, Vol. 41, No. 6, 20 February 2002, pp. 1012-1021.
[5] Kelly, B.O., "Lateral-Effect Photodiodes," Laser Focus, Mar. 1976, pp. 38-40

The motivation for a new S-H sensor verson 2 is to study different sensing method, as per Siegenthaler's above thesis, and to see how well the telescope blur spot is corrected before making an investment of time and money to build a tip/tilt servo system. Inevitably such a tip/tilt servo will be imperfect and it is valuable to understand these errors before building the servo. As seen from Siegenthaler's Ph.D. dissertation there are subelties in sensing methods that need to be explored. To that end, this S-H sensor version 2 provides not only the S-H spots for wavefront analysis, but also the telescope's blur spot.

To that end the original version 1 of the S-H sensor design that is detailed in Astronomy Notebook pg 1, April 26, 2014, with diffraction effects given on pg 10, April 27, 2014, is modified by adding two beam splitters that bypass the S-H lenslet array and send its light directly to the focal plane. To avoid the difficulties of having two camera focal planes that need to be time synchronized and their attendant increase of data rate into the processing CPU, the design only uses one focal plane.